

SLOWLY MODULATED TWO-PULSE SOLUTIONS IN THE GRAY–SCOTT MODEL I: ASYMPTOTIC CONSTRUCTION AND STABILITY*

ARJEN DOELMAN[†], WIKTOR ECKHAUS[‡], AND TASSO J. KAPER[§]

With great sadness, we note the passing away of our mentor and colleague Wiktor.

Abstract. Two pulse solutions play a central role in the phenomena of self-replicating pulses in the one-dimensional (1-D) Gray–Scott model. In the present work (part I of two parts), we carry out an existence study for solutions consisting of two symmetric pulses moving apart from each other with slowly varying velocities. This corresponds to a “mildly strong” pulse interaction problem in which the inhibitor concentration varies on long spatial length scales. Critical maximum wave speeds are identified, and ODEs are derived for the wave speed and for the separation distance between the pulses. In addition, the formal linear stability of these two-pulse solutions is determined. Good agreement is found between these theoretical predictions and the results from numerical simulations. The main methods used in this paper are analytical singular perturbation theory for the existence demonstration and the nonlocal eigenvalue problem (NLEP) method developed in our earlier work for the stability analysis. The analysis of this paper is continued in [A. Doelman, W. Eckhaus, and T. Kaper, *SIAM J. Appl. Math.*, to appear], where we employ geometric methods to determine the bifurcations of the slowly modulated two-pulse solutions. In addition, in Part II we identify and quantify the central role of the slowly varying inhibitor concentration for two-pulse solutions in determining pulse splitting, and we answer some central questions about pulse splitting.

Key words. reaction-diffusion equations, modulated traveling waves, singular perturbation theory, self-replicating patterns

AMS subject classifications. 35K57, 35B25, 35B32, 35B40, 34C37, 92E20

PII. S0036139999354923

1. Introduction. Self-replicating spots and pulses have been observed in excitable reaction-diffusion systems [18, 14, 20, 19, 13, 9, 2, 3, 4, 21, 17, 16, 15, 8]. Spots and pulses are regions in which the concentrations of some of the species exhibit large amplitude perturbations from a surrounding homogeneous state. Depending on system parameters, these regions can enlarge and split so that the spots and pulses replicate in a complex, and as yet incompletely understood, manner.

Two-pulse patterns play a fundamental role in the phenomenon of pulse splitting in one-dimensional (1-D) systems; see [20, 19, 2, 17]. To understand this phenomenon, it is necessary to study the evolution of solutions consisting of pairs of pulses in which the pulses move apart from each other; see Figure 1. Outside the parameter domain in which the splitting process takes place, the pulses settle down, eventually, in a stationary two-pulse pattern (on a bounded domain). See Figure 2(a). In the critical regime where splitting is first observed, the two pulses (or spikes) are observed to

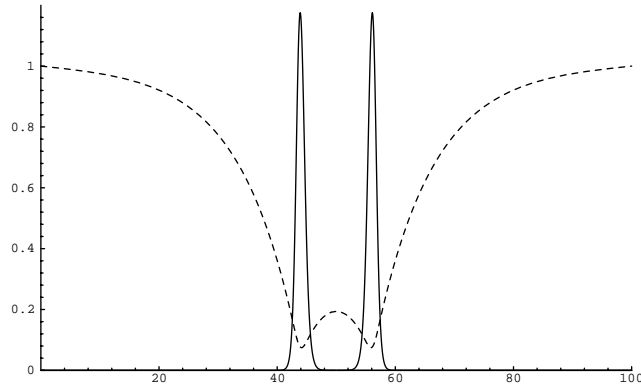
*Received by the editors April 26, 1999; accepted for publication (in revised form) April 10, 2000; published electronically October 31, 2000.

<http://www.siam.org/journals/siap/61-3/35492.html>

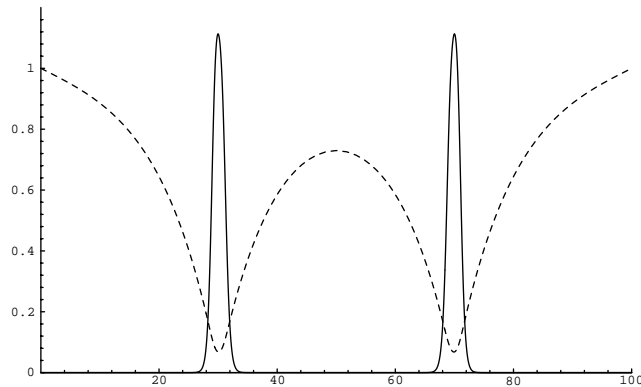
[†]Korteweg-deVries Instituut, Universiteit van Amsterdam, Plantage Muidergracht 24, 1018TV Amsterdam, the Netherlands (doelman@wins.uva.nl). The research of this author was supported by the Organization for Scientific Research (NWO).

[‡]The author is deceased. Former address: Mathematisch Instituut, Universiteit Utrecht, P.O. Box 80.010, 3508TA Utrecht, The Netherlands (eckhaus@math.uu.nl).

[§]Department of Mathematics and Center for BioDynamics, Boston University, 111 Cummington Street, Boston, MA 02215 (tasso@math.bu.edu). The research of this author was supported by the National Science Foundation through CAREER grant DMS-9624471 and a Sloan Research Fellowship (1995–1998).



(a)



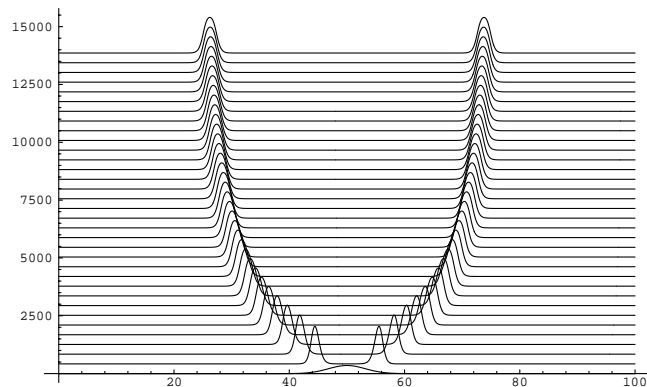
(b)

FIG. 1. (a) A two-pulse solution shown at time $t = 500$ obtained from numerical simulations of the PDE (1.1) with $A = 0.01$, $B = 0.0696$, and $D = 0.01$. The U component is shown dashed, with U reaching a local maximum in between the V pulses (solid curve) at $U_{\max} \approx 0.194$. The two pulses move apart from each other with slowly varying speeds $c(t)$, and the U component is an $\mathcal{O}(1)$ distance away from the homogeneous state in between the pulses, even though the pulses are quite far apart. (b) The solution (U, V) from the same initial data shown at a later time ($t = 5,000$), and the value of U_{\max} has slowly risen to ≈ 0.730 .

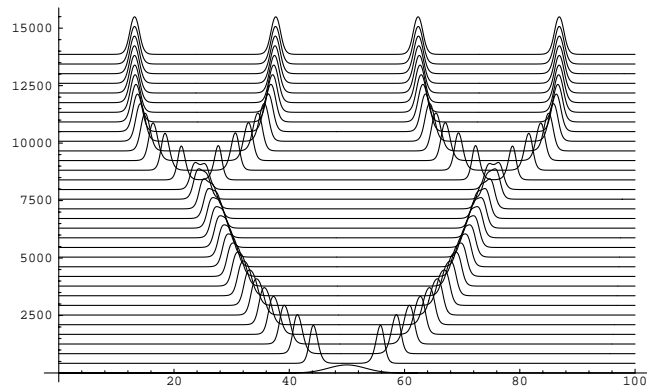
move apart from each other with a slowly decreasing velocity and then to undergo the splitting process when they are nearly stationary. See Figure 2(b). Further from critical, the pulses are observed to propagate with constant speed in between successive splittings.

In this work, we carry out an existence and stability analysis for two-pulse patterns in the irreversible 1-D Gray–Scott model [10] (see also the references in [10, 18, 19, 2] for the derivations and early studies of this model):

$$(1.1) \quad \frac{\partial U}{\partial t} = \frac{\partial^2 U}{\partial x^2} - UV^2 + A(1 - U), \quad \frac{\partial V}{\partial t} = D \frac{\partial^2 V}{\partial x^2} + UV^2 - BV.$$



(a)



(b)

FIG. 2. (a) Time evolution of the V component of a modulating two-pulse solution of (1.1) with $A = 0.01$, $B = 0.0696$, and $D = 0.01$, i.e., below $\varepsilon_{\text{split}}$. (b) A numerical simulation of pulse splitting in (1.1), showing V pulses with slowly decreasing speeds which split when the speeds are small. The parameter values are $A = 0.01$, $B = 0.0674$, and $D = 0.01$. In both plots, the vertical axis is $1,400V + t$ (where by default we use $T_{\text{end}}/10$ as the multiple of V), and $L = 100$.

For all positive values of the parameters A , B , and D , the background homogeneous state ($U \equiv 1$, $V \equiv 0$) is stable. The two-pulse solutions considered here are asymptotic to it as $x \rightarrow \pm\infty$. The pulses correspond to excursions of the V -components away from $V \equiv 0$ on narrow intervals in which U is approximately constant. Outside of these intervals, U varies significantly, while V is exponentially small.

We focus here on solutions of (1.1) in which the pulses are symmetric about $x = 0$. Motivated by numerical simulations (see Figures 1 and 2), we specifically allow the pulse velocities, $-c(t)$ and $c(t)$, to vary slowly in time. We find that the slowly varying wave speeds $c(t)$ are determined self-consistently by certain ODEs that give the time courses of both $c(t)$ and $2\Gamma(t)$, the separation distance between the two pulses. The

speeds scale as $A\sqrt{D}/B^{3/2}$, in agreement with the numerical simulations in [2] and those carried out here. Furthermore, the ODEs predict an algebraic rate of decay to zero as $t \rightarrow \infty$, in agreement with time courses observed numerically.

Two parameter groups, \sqrt{A}/B and \sqrt{BD} , arise naturally from scaling analysis of (1.1), and they were already identified, for instance, in [11] in a different parameter regime from that studied here. In this paper, our construction of the slowly modulated two-pulse solutions is carried out with the primary conditions

$$(1.2) \quad A/B^2 \ll 1 \quad \text{and} \quad B^3 D/A \leq \mathcal{O}(1).$$

The first condition in (1.2) corresponds to the case in which the spatial rates of change of U and its first spatial derivative are significantly slower than those of V and its first spatial derivative. Therefore, in this primary regime, there is an asymptotic separation that we exploit in the construction. Moreover, the second ratio in (1.2), related to the ratio of the second and first parameter groups, corresponds to the square of the relative size of U at the pulse center.

It turns out, however, that the first condition in (1.2) is sufficient but not necessary. The slowly modulated two-pulse solutions *also exist* on the boundary:

$$(1.3) \quad A/B^2 = \mathcal{O}(1),$$

and the other condition in (1.2) holds. However, the technique needed to demonstrate this is different, since there is no longer a natural separation of time scales for the dependent variables. In fact, our work with a topological shooting method in [3], in which we establish the existence of stationary pulse solutions, extends to show that modulating two-pulse solutions also exist when (1.3) holds. Moreover, that same analysis also applies nearly verbatim to show that there is a critical curve in this scaling such that the two-pulse solutions do not exist on the other side, a curve called a disappearance bifurcation for the stationary pulse solutions in [3]. Therefore, there is a large, closed parameter region in which these solutions exist.

The existence analysis in this work is formulated in the framework of a leading order quasi-stationary approximation. In particular, focusing first on the right-traveling pulse on the half-line $x \geq 0$, we work in a moving coordinate system given by $\xi(t) = x - \Gamma(t)$, where $x = \Gamma(t)$ is the time-dependent location of the pulse's center. In this coordinate system, the leading order quasi-stationary approximation entails assuming that the solutions $(U(\xi(t), t), V(\xi(t), t))$ depend only on t through $\xi(t)$. Hence, it is assumed that $c(t)$ is a slowly varying parameter and that the explicit time derivatives of U and V are neglected to leading order. This solution on the right semi-infinite line $x \geq 0$ is then reflected to obtain also the solution for the left-moving pulse on $x \leq 0$. Moreover, by including higher order terms, it can be shown (see section 3.4 of Part II of this paper [1]) that these two pieces hook up smoothly and that the entire quasi-stationary approximation method is self-consistent.

In this paper, we also study the linear stability of the slowly modulating two-pulse solutions using the nonlocal eigenvalue problem (NLEP) method developed in [3]. We find that the two-pulse solutions undergo subcritical Hopf bifurcations at a certain critical parameter combination, $\mathcal{C}_{\text{HOPF}}$, for $A = \mathcal{O}(B^2\sqrt{D})$. For parameter combinations above $\mathcal{C}_{\text{HOPF}}$, the solutions are (formally) linearly stable with respect to perturbations that evolve on time scales that are shorter than that of the rate of change of $c = c(t)$, while for parameters just below $\mathcal{C}_{\text{HOPF}}$, their instability is manifested by large-scale oscillations in the pulse amplitudes. The NLEP method was developed in [3] to analyze the stability of the stationary one-pulse patterns of (1.1) in the special

scaling of [2] (see also Remark 2.2 below). Moreover, the validity of this method for stationary solutions has been established by a stability index analysis in [4], and [5] showed that this method applies to many reaction-diffusion (R-D) equations.

The slowly modulated two-pulse solutions constructed in this paper and their continuations into the splitting regime where $A/B^2 = \mathcal{O}(1)$ play central roles in the splitting and self-replication processes. One aspect of this role is studied here in section 3.4. In particular, it is shown here that, as the ratio A/B^2 approaches the critical regime in which it becomes $\mathcal{O}(1)$, the structure of the slowly modulating two-pulse solutions naturally suggests a possible mechanism for their splitting. In Part II of this work (see [1]), the role of these two-pulse solutions in pulse splitting is further quantified and explained. It is shown there that the two-pulse solutions can be interpreted as governing the transition between a one-pulse solution that has just split into two and a time-asymptotic state in the splitting regime, which is a stable stationary periodic multipulse pattern. See Figure 2(b) and [20, 19, 2, 21, 3, 17, 16]. In particular, we analyze the dynamics of the slowly varying U component in between the pulses.

In Part II, we also use geometric singular perturbation theory to identify the saddle node bifurcations in which the slowly modulated two-pulse solutions constructed here are created and annihilated, as well as to determine the bifurcations they undergo to traveling waves with constant wave speed. Moreover, it is shown in Part II that the geometric theory also provides a natural interpretation of the critical (maximum) allowable speeds $c(t)$ found here. Finally, in Part II, we relate the results obtained in both Parts I and II to the literature, especially [20, 21, 17].

Overall, our study of slowly modulating pulses in Parts I and II of this work may be classified as a treatment of the “mildly strong” pulse interaction problem. A crucial aspect of the analysis here is that the “slow” U component undergoes $\mathcal{O}(1)$ changes away from $U \equiv 1$ over large intervals on both sides of a pulse; see Figure 1. Weak pulse interactions, by contrast, occur when both the U and the V components are close to the background, homogeneous, stable state in between the two pulses (see, for instance, [8]). The case of weak pulse interactions can be obtained from the analysis here by taking the limit $t \rightarrow \infty$, so that the pulses are so far apart that $U \approx 1$ in between.

This paper is organized as follows. Sections 2 and 3 contain the analytical perturbation method for stationary one-pulse solutions and slowly modulating two-pulse solutions, respectively. The linear stability analysis of the two-pulse solutions is presented in section 4. Finally, in section 5, we compare to the weak interaction problem.

Remark 1.1. The conditions (1.2) are the most important conditions on the parameters A , B , and D of (1.1). There is one additional condition, $D \ll 1$, that will appear in the stability analysis of section 4 here and in the validity analysis of section 3.4 of Part II [1]. The case $D \geq \mathcal{O}(1)$ turns out to be of little interest since here the pulse solutions cannot be stable; see Remark 4.2. Note, however, that there certainly are stable “localized” patterns for $D = \mathcal{O}(1)$ in a parameter regime that differs from the regime studied here, $AD = \mathcal{O}(B^2)$ (conditions (1.2) implies that $AD \ll B^2$); see [11, 12] for the case $AD = B^2$, $D = 1$.

2. Stationary single-pulse solutions. We present an asymptotic analysis of the stationary single-pulse solutions of the PDE (1.1); see Figure 3. The existence of these solutions was proven in [2] for a special choice of parameters using methods from geometric singular perturbation theory. Our purposes here are to briefly revisit the existence result from a different perspective, to derive the broader scalings for

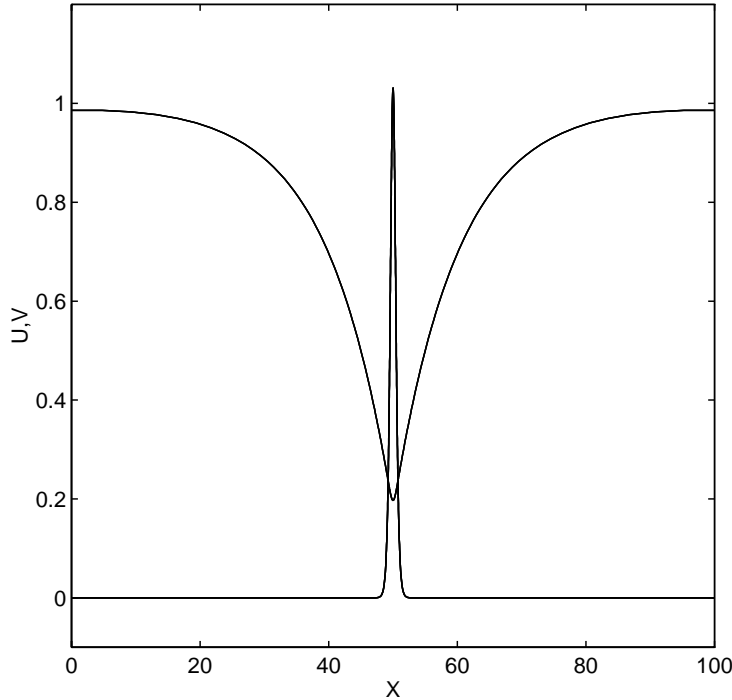


FIG. 3. A stationary one-pulse solution of (1.1) whose existence is demonstrated in section 2 and in [2]. The parameter values are $A = 0.01$, $B = 0.1423$, and $D = 0.01$.

which pulse solutions exist, and to preview the method that will be used in section 3 on the full problem. The extension of the existence results was briefly announced in Remark 1.1 of [3] (see also [16] for a construction of the stationary spikes).

2.1. Analytical perturbation theory. Stationary solutions of (1.1) are functions $(u(x), v(x))$ for $x \in \mathbb{R}$ satisfying the coupled ODEs

$$(2.1) \quad \frac{\partial^2 u}{\partial x^2} - uv^2 + A(1 - u) = 0, \quad D \frac{\partial^2 v}{\partial x^2} + uv^2 - Bv = 0.$$

$A, B,$ and D are independent parameters. Eventually, it will be useful to make choices about their orders of magnitude, but we postpone this as long as possible.

Let $u_0 \equiv [u]_{x=0}$ be the value of u at the center of the pulse (see Figure 1). The v -problem for the pulse is made more transparent by introducing new variables

$$(2.2) \quad \hat{\xi} = \sqrt{\frac{B}{D}}x \quad \text{and} \quad \hat{v}(\hat{\xi}) = \frac{u_0}{B}v(x).$$

Hence,

$$(2.3) \quad \frac{\partial^2 \hat{v}}{\partial \hat{\xi}^2} + \left(\frac{u(x)}{u_0} \right) \hat{v}^2 - \hat{v} = 0.$$

The main goal is to determine the values of u_0 for which stationary single-pulse solutions exist, and the basis of the analytic approximation method to be developed in this section is that there is a disparity between the rates of change of u and v . We

will see that \hat{v} varies on an $\mathcal{O}(1)$ interval in the $\hat{\xi}$ variable, while significant variation in u only occurs over much longer intervals.

The first step in the analytical method is to derive an approximation for $u(x)$ along a single-pulse solution. Treating $v(x)$ in (2.1) as if it were a known function, and putting the v term on the right-hand side, one gets, by a standard procedure,

$$(2.4) \quad u(x) = 1 - \frac{1}{2\sqrt{A}} \left\{ \int_{-\infty}^x e^{\sqrt{A}(x'-x)} u(x') v^2(x') dx' + \int_x^{\infty} e^{\sqrt{A}(x-x')} u(x') v^2(x') dx' \right\}.$$

Formula (2.4) is an integral equation for $u(x)$ that may be solved for a given $v(x)$. A pulse-like function $v^2(x)$ should be expected to have a substantial magnitude inside the pulse interval, which is an order $\sqrt{D/B}$ neighborhood of the origin (by virtue of (2.2) and (2.3)), and it should be virtually zero for x outside this same neighborhood. Also, inside this neighborhood, the functions $u(x')$ and $e^{\pm\sqrt{A}x'}$ are assumed to be slowly varying (see the end of this section for a consistency condition), and it suffices to keep the first (constant) term in their Taylor expansions about $x' (= \hat{\xi}) = 0$ in order to obtain the leading order terms for the integrals in (2.4). Hence,

$$(2.5) \quad u(x) = 1 - \frac{u_0}{2\sqrt{A}} \left\{ e^{-\sqrt{A}x} \int_{-\infty}^x v^2(x') dx' + e^{\sqrt{A}x} \int_x^{\infty} v^2(x') dx' \right\}.$$

Higher order terms in an asymptotic expansion for $u(x)$ can be constructed by iteration and by Taylor expanding $u(x')$ and the exponential functions in the integrals.

This first approximation (2.5) can be simplified one step further by evaluating the integrals. Since $v(x)$ is insignificant outside a vanishingly small interval about $x = 0$, the integrals are given to leading order asymptotically by the integrals over the entire real line. Hence,

$$(2.6) \quad u(x) \sim 1 - \frac{k u_0}{2\sqrt{A}} e^{\sqrt{A}x} \text{ for } x < 0; \quad u(x) \sim 1 - \frac{k u_0}{2\sqrt{A}} e^{-\sqrt{A}x} \text{ for } x > 0,$$

$$(2.7) \quad k = \int_{-\infty}^{\infty} v^2(x') dx'.$$

Note that the v -component acts as a delta function in this approximation. Finally, evaluating (2.5) at $x = 0$, one obtains $u_0 = 1 - \frac{k u_0}{2\sqrt{A}}$. Hence, for a given k

$$(2.8) \quad u_0 = \frac{2\sqrt{A}}{2\sqrt{A} + k}.$$

Thus, the values of the unknown u_0 that correspond to stationary single-pulse solutions can be determined when one knows the associated values of the integral k .

In this second step, we derive an approximation for the $v(x)$ component of a single-pulse solution that will in turn enable us to determine k . Write (2.3) as

$$(2.9) \quad \frac{\partial^2 \hat{v}}{\partial \hat{\xi}^2} + \hat{v}^2 - \hat{v} = \left[\frac{u_0 - u(x)}{u_0} \right] \hat{v}^2.$$

The function $u(x)$ varies little near u_0 within the region of the pulse $\hat{\xi} = \mathcal{O}(1)$, so that the right-hand side of (2.9) acts as a perturbation. This suggests approximating

$\hat{v}(\hat{\xi})$ by the function

$$(2.10) \quad \hat{v}_0(\hat{\xi}) = \frac{3}{2} \operatorname{sech}^2 \left(\frac{\hat{\xi}}{2} \right),$$

which is the solution of $(\partial^2 \hat{v}_0 / \partial \hat{\xi}^2) + \hat{v}_0^2 - \hat{v}_0 = 0$, with $\hat{v}_0 \rightarrow 0$ as $\hat{\xi} \rightarrow \pm\infty$.

Substituting (2.10) into (2.7) and recalling (2.2), one finds

$$(2.11) \quad k = 6 \frac{B^{3/2} \sqrt{D}}{u_0^2}.$$

Hence, by (2.8), the allowable u_0 for stationary one-pulse solutions are given by

$$(2.12) \quad u_0(1 - u_0) = 3 \frac{B^{3/2} \sqrt{D}}{\sqrt{A}}.$$

Upon examining (2.12) for u_0 , one sees that there are two cases to consider.

Case I: $B^{3/2} \sqrt{D/A} \ll 1$; Case II: $B^{3/2} \sqrt{D/A} = \mathcal{O}(1)$ and $B^{3/2} \sqrt{D/A} < 1/12$.
 (2.13)

In Case I, we may Taylor expand both roots of the quadratic (2.12). One solution is

$$(2.14) \quad u_0 \sim 3B \sqrt{BD/A}.$$

Clearly, in this case, u_0 is asymptotically small, and it is precisely in this case that the existence of one-pulse stationary solutions was proven for a special scaling of A, B , and D in Theorem 4.1 of [2]; see Remark 2.2 below. Moreover, in [3] these solutions were shown to be stable, gaining their stability through a Hopf bifurcation, in a large region of the parameter space.

Remark 2.1. The other root corresponds to a “weak” pulse solution with maximum value for $v(x)$ of $\mathcal{O}(B)$. We expect that this “weak” pulse is unstable, since with $u_0 \sim 1 - 3B \sqrt{BD/A}$, it is a small perturbation of the globally stable homogeneous steady state ($U = 1, V = 0$).

In Case II, both roots of (2.12) are $\mathcal{O}(1)$. The existence of the two associated stationary single-pulse solutions was established in Theorem 4.3 of [2], and both have peaks of height $\mathcal{O}(B)$. Moreover, it was shown (again in the special scaling, though the same analysis can be carried out here) in Theorem 4.3 of [2] that they are born in a saddle node bifurcation when $B \sqrt{BD/A} = 1/12$.

Having shown how to construct the stationary solutions with $u(x = 0) = u_0$ in both Cases I and II, we conclude by showing that the perturbation analysis is self-consistent. An important condition emerges that will be imposed globally, except where noted, in the rest of the paper. If one scales the u variable by the size of u_0 (2.14), $u = B^{3/2} \sqrt{D/A} \hat{u}$, and then substitutes this scaling and those (2.2) of ξ and v into the quasi-stationary ODE for u , one gets

$$(2.15) \quad \frac{\partial^2 \hat{u}}{\partial \hat{\xi}^2} = \frac{A}{B^2} \left[\hat{u} \hat{v}^2 - \frac{A}{\sqrt{B}} (1 - B^{3/2} \hat{u}) \right].$$

Hence, we must impose the following global condition so that \hat{u} evolves slowly:

$$(2.16) \quad \frac{A}{B^2} \ll 1.$$

Hence, \hat{u} evolves slowly in $\hat{\xi}$ relative to the $\mathcal{O}(1)$ rate of change of \hat{v} .

Remark 2.2. In order to compare our results with [2], we set (for this remark only) $D = \delta^2$, where $0 < \delta \ll 1$, $A = \delta^2 a$, and $B = \delta^{2\alpha/3} b$ with $\alpha = 1$ ($\alpha \in [0, 3/2]$ in the analysis in [2], $\alpha = 1$ in most of the numerical simulations in [2]). With these special relations, one solution of (2.12) is $u_0 = (3B^{3/2}/\sqrt{a})\delta[1 + \mathcal{O}(B^{3/2})]$. The corresponding “strong” pulse is then approximated by $v(x) = (1/3)\sqrt{a/B}\delta^{-1/3}\hat{v}_0(\xi)$. For this solution, u_0 is small, and the maximum value of $v(x)$ is large. The results of the asymptotic analysis carried out here for this pulse solution fully agree with the results of Theorem 4.1 in [2], obtained by geometric methods and the Fenichel theory.

Remark 2.3. The heuristic approximations (2.5) and (2.10) can be made rigorous, under a number of conditions on A, B , and D , by converting the full problem (2.9) into an integral equation. Setting $\hat{v} = \hat{v}_0 + \hat{v}_1$, it follows that \hat{v}_1 satisfies the ODE

$$(2.17) \quad \left(\frac{\partial^2}{\partial \hat{\xi}^2} + 2\hat{v}_0(\hat{\xi}) - 1 \right) \hat{v}_1 = \frac{u_0 - u(x)}{u_0} (\hat{v}_0 + \hat{v}_1)^2 - \hat{v}_1^2 \equiv \mathcal{R}(\hat{v}_0, \hat{v}_1).$$

Letting $G(\hat{\xi}, \hat{\xi}')$ denote the Green’s function (computed explicitly from the solutions $\psi_1(\hat{\xi}) = (d\hat{v}_0/d\hat{\xi})(\hat{\xi})$ and $\psi_2(\hat{\xi})$ of the homogeneous equation) (2.17) is equivalent to

$$(2.18) \quad \hat{v}_1(\hat{\xi}) = \int_{-\infty}^{\infty} G(\hat{\xi}, \hat{\xi}') \mathcal{R}(\hat{v}_0(\hat{\xi}'), \hat{v}_1(\hat{\xi}')) d\hat{\xi}'.$$

Higher approximations for $\hat{v}(\hat{\xi})$ can be computed iteratively from this integral equation. Furthermore, viewing (2.4) and (2.18) as a pair of integral equations, one can envision the proof of validity of the first approximations (2.5) and (2.10) by using the contraction mapping principle in a suitably defined Banach space. Such techniques have been used successfully in other nonlinear problems in [7] and [22]; see [22] for a general development of the method.

2.2. The effects of a finite interval for a stationary single pulse. In [2], the numerical simulations were done on a finite interval, say, $x \in [-L, L]$, and it was shown experimentally that, if the interval is large enough, changing the length does not affect the numerical solution.

We analyze here the finite-interval problem (with Dirichlet boundary conditions) by the same method used in section 2.1. The main task is to solve the equation (2.1) for $u(x)$ with boundary conditions $u = 1$ for $x = \mp L$. This is an elementary exercise, but the formulas are lengthy. We introduce the abbreviation

$$f(x') = u(x')v^2(x').$$

Instead of (2.4), one gets

$$(2.19) \quad u(x) = 1 - \frac{1}{2\sqrt{A}} \left\{ e^{-\sqrt{A}x} \left[C_1 + \int_{-L}^x e^{\sqrt{A}x'} f(x') dx' \right] + e^{\sqrt{A}x} \left[C_2 + \int_x^L e^{-\sqrt{A}x'} f(x') dx' \right] \right\},$$

$$(2.20) \quad C_1 = \frac{1}{2\sinh 2L\sqrt{A}} \left[e^{-2L\sqrt{A}} \int_{-L}^L e^{\sqrt{A}x'} f(x') dx' - \int_{-L}^L e^{-\sqrt{A}x'} f(x') dx' \right],$$

$$(2.21) \quad C_2 = \frac{1}{2\sinh 2L\sqrt{A}} \left[e^{-2L\sqrt{A}} \int_{-L}^L e^{-\sqrt{A}\varepsilon x'} f(x') dx' - \int_{-L}^L e^{\sqrt{A}x'} f(x') dx' \right].$$

In terms of the same approximations used in section 2.1, these formulas greatly simplify. One obtains $C_2 = C_1$, where

$$(2.22) \quad C_1 = \frac{ku_0}{2\sinh 2L\sqrt{A}} \left[e^{-2L\sqrt{A}} - 1 \right].$$

Furthermore,

$$u(x) \cong 1 - \frac{1}{2\sqrt{A}} \left\{ e^{-\sqrt{A}x} \left[C_1 + \int_{-L}^x v^2(x') dx' \right] + e^{\sqrt{A}x} \left[C_2 + \int_x^L v^2(x') dx' \right] \right\}.$$

Thus, we directly find the following leading order result for u_0 :

$$(2.23) \quad u_0 = 1 - \frac{ku_0}{2\sqrt{\varepsilon}} \left[1 + \frac{e^{-2L\sqrt{A}} - 1}{\sinh 2L\sqrt{A}} \right].$$

Therefore, when L is large enough, the correction due to the finite interval is exponentially small. In addition, we performed numerical simulations of (1.1) for this paper with the typical values $A = \mathcal{O}(D) \ll 1$ and $2L = 100$, so that $2L\sqrt{A} = \mathcal{O}(1/\sqrt{D}) \gg 1$. All of these simulations confirmed that the effect of having a finite (as opposed to an infinite) interval was indeed negligible. Finally, the simulations reported in [20, 2, 21, 3] are also consistent with this analysis.

3. Traveling two-pulse solutions. In this section, we present the analytical perturbation theory for the slowly modulated two-pulse solutions for which $c(t)$ is a slowly varying function of t .

3.1. The quasi-stationary approximation. Because of the symmetry about $x = 0$, the analysis can be restricted to half the picture (however, see section 3.4 of Part II). We chose the right-moving pulse on $x > 0$ (see Figure 1). At time t , the center of the pulse is at

$$(3.1) \quad x = \Gamma(t), \quad \text{where } \Gamma(t) = \int_0^t c(s) ds.$$

We also introduce a coordinate attached to the pulse

$$(3.2) \quad \xi = x - \Gamma(t).$$

By (1.1), the equation and boundary conditions for $U(\xi(t), t)$ take the form

$$(3.3) \quad \frac{\partial U}{\partial t} - c \frac{\partial U}{\partial \xi} = \frac{\partial^2 U}{\partial \xi^2} - UV^2 + A(1 - U),$$

$$(3.4) \quad U \rightarrow 1 \quad \text{as } \xi \rightarrow \infty \quad \text{and} \quad \frac{\partial U}{\partial \xi} = 0 \quad \text{for } \xi = -\Gamma(t).$$

The second condition in (3.4) arises due to the symmetry of the full problem for $x \in (-\infty, \infty)$: here the right-moving pulse must “match” with the left-moving pulse.

The quasi-stationary approximation consists of imposing the *ansatz* that the solution $(U(\xi(t), t), V(\xi(t), t))$ depends only on t through $\xi(t)$: $(U(\xi(t), t), V(\xi(t), t)) = (u(\xi(t)), v(\xi(t)))$, where (u, v) does not depend explicitly on t . Thus, the derivative $\frac{\partial U}{\partial t}$ disappears from (3.3): the equation for u is an ODE in which t is a parameter that appears in $c = c(t)$ and in the position of the boundary condition (3.4). We will see that the construction of singular solutions (in the spirit of the previous section) will imply a relation between $c(t)$ and $\Gamma(t) = \int_0^t c(s) ds$.

In the quasi-stationary approximation, the equation for $v(\xi)$ becomes

$$(3.5) \quad -c \frac{\partial v}{\partial \xi} = D \frac{\partial^2 v}{\partial \xi^2} + uv^2 - Bv.$$

As in section 2, this equation becomes transparent in the new variables (2.2). Recall

$$(3.6) \quad \hat{\xi} = \sqrt{\frac{B}{D}} \xi, \quad \hat{v}(\hat{\xi}, t) = \frac{u_0}{B} v(\xi, t),$$

where u_0 is again u at $\xi = 0$, but now u_0 depends on the “parameter” time. Hence,

$$(3.7) \quad \frac{-c}{\sqrt{BD}} \frac{\partial \hat{v}}{\partial \hat{\xi}} = \frac{\partial^2 \hat{v}}{\partial \hat{\xi}^2} + \left(\frac{u}{u_0}\right) \hat{v}^2 - \hat{v}.$$

We look for pulse-like solutions for $\hat{v}(\hat{\xi}, t)$, i.e., solutions that tend rapidly to zero when $|\hat{\xi}|$ is large. Hence, the boundary condition for all t is $\hat{v}(\hat{\xi}, t) \rightarrow 0$ as $|\hat{\xi}| \rightarrow \infty$.

3.2. Approximate solutions for $u(\xi)$. Let

$$(3.8) \quad \mu_{\pm} \equiv \frac{1}{2} \left(-c \pm \sqrt{c^2 + 4A} \right),$$

and note for later reference that when $c^2 \ll A$,

$$(3.9) \quad \mu_{\pm} \sim \pm \sqrt{A}.$$

The general solution of (3.3) in the quasi-stationary limit is now at hand by elementary procedures:

$$(3.10) \quad u(\xi) = 1 - \frac{1}{(\mu_+ - \mu_-)} \left\{ e^{\mu_- \xi} \int_{-\Gamma(t)}^{\xi} e^{-\mu_- x'} u(x') v^2(x') dx' \right. \\ \left. + e^{\mu_+ \xi} \int_{\xi}^{\infty} e^{-\mu_+ x'} u(x') v^2(x') dx' \right. \\ \left. - \frac{\mu_+}{\mu_-} e^{(\mu_- - \mu_+) \Gamma(t)} e^{\mu_- \xi} \int_{-\Gamma(t)}^{\infty} e^{-\mu_+ x'} u(x') v^2(x') dx' \right\}.$$

Matters simplify considerably when one observes, as in section 2, that the pulse-like function $v(x')$ is expected to be virtually zero outside an $\mathcal{O}(\sqrt{D/B})$ neighborhood of $x' = 0$. Taylor expanding $u(x')$ and the exponential functions, one obtains

$$(3.11) \quad u(\xi) \sim 1 - \frac{u_0}{(\mu_+ - \mu_-)} \left\{ e^{\mu_- \xi} \int_{-\Gamma}^{\xi} v^2(x') dx' + e^{\mu_+ \xi} \int_{\xi}^{\infty} v^2(x') dx' \right. \\ \left. - \frac{\mu_+}{\mu_-} e^{(\mu_- - \mu_+) \Gamma} e^{\mu_- \xi} \int_{-\Gamma}^{\infty} v^2(x') dx' \right\}.$$

As noted in Remark 2.3, one can envision a procedure for the construction of higher approximations. Fortunately, the results of Part II make this unnecessary.

For values of ξ outside the small interval where $v(\xi)$ is nonzero, further simplification follows:

$$(3.12) \quad u(\xi) \sim 1 - \frac{ku_0}{(\mu_+ - \mu_-)} \left\{ e^{\mu-\xi} - \left(\frac{\mu_+}{\mu_-} \right) e^{(\mu_- - \mu_+) \Gamma(t)} e^{\mu-\xi} \right\} \quad \text{for } \xi > 0,$$

$$(3.13) \quad u(\xi) \sim 1 - \frac{ku_0}{(\mu_+ - \mu_-)} \left\{ e^{\mu+\xi} - \left(\frac{\mu_+}{\mu_-} \right) e^{(\mu_- - \mu_+) \Gamma(t)} e^{\mu-\xi} \right\} \quad \text{for } \xi < 0,$$

where, as before,

$$(3.14) \quad k = \int_{-\infty}^{\infty} v^2(x') dx'.$$

Finally, by evaluating (3.11) at $\xi = 0$, it also follows that to leading order

$$(3.15) \quad u_0 = 1 - \frac{ku_0}{(\mu_+ - \mu_-)} \left\{ 1 - \left(\frac{\mu_+}{\mu_-} \right) e^{(\mu_- - \mu_+) \Gamma(t)} \right\},$$

which relates the unknown u_0 and the integral k , which is also unknown at this stage.

3.3. Approximate solutions for $\hat{v}(\hat{\xi})$. Following the same procedure used in section 2 for the stationary single-pulse solutions, we now develop an approximation for the v -component of a slowly modulated, traveling single pulse. We begin by rewriting the problem (3.7) in the quasi-stationary approximation:

$$(3.16) \quad \frac{\partial^2 \hat{v}}{\partial \hat{\xi}^2} + \hat{v}^2 - \hat{v} = \left(\frac{u_0 - u}{u_0} \right) \hat{v}^2 - \frac{c}{\sqrt{BD}} \frac{\partial \hat{v}}{\partial \hat{\xi}} \quad \text{with } \hat{v} \rightarrow 0 \quad \text{as } |\hat{\xi}| \rightarrow \infty.$$

The full equation (3.16) is *not* invariant under the transformation $\hat{\xi} \rightarrow -\hat{\xi}$, and therefore, the existence of solutions that tend to zero for $\hat{\xi} \rightarrow -\infty$ and $\hat{\xi} \rightarrow +\infty$ is a nontrivial matter. To see this more clearly, we compute an integral of (3.16), as follows. Multiplication by $\partial \hat{v} / \partial \hat{\xi}$ yields

$$(3.17) \quad \frac{1}{2} \frac{\partial}{\partial \hat{\xi}} \left(\frac{\partial \hat{v}}{\partial \hat{\xi}} \right)^2 + \frac{1}{3} \frac{u}{u_0} \frac{\partial (\hat{v}^3)}{\partial \hat{\xi}} - \frac{1}{2} \frac{\partial (\hat{v}^2)}{\partial \hat{\xi}} = \frac{-c}{\sqrt{BD}} \left(\frac{\partial \hat{v}}{\partial \hat{\xi}} \right)^2.$$

Next, we integrate (3.17) and impose the boundary condition in (3.16) for $\hat{\xi} \rightarrow +\infty$:

$$(3.18) \quad \frac{1}{2} \left(\frac{\partial \hat{v}}{\partial \hat{\xi}} \right)^2 + \frac{u \hat{v}^3}{3u_0} - \frac{\hat{v}^2}{2} = \frac{-c}{\sqrt{BD}} \int_{\hat{\xi}}^{\infty} \left(\frac{\partial \hat{v}}{\partial \hat{\xi}} \right)^2 d\hat{\xi} + \frac{1}{3} \int_{\hat{\xi}}^{\infty} \hat{v}^3 \frac{\partial}{\partial \hat{\xi}} \left(\frac{u}{u_0} \right) d\hat{\xi}.$$

Finally, by imposing the boundary condition in (3.16) for $\hat{\xi} \rightarrow -\infty$, one obtains the following nontrivial condition for the existence of a homoclinic orbit:

$$(3.19) \quad \frac{-c}{\sqrt{BD}} \int_{-\infty}^{\infty} \left(\frac{\partial \hat{v}}{\partial \hat{\xi}} \right)^2 d\hat{\xi} + \frac{1}{3} \int_{-\infty}^{\infty} \hat{v}^3 \frac{\partial}{\partial \hat{\xi}} \left(\frac{u}{u_0} \right) d\hat{\xi} = 0.$$

In the analysis here we treat the right-hand side of (3.16) as a perturbation and approximate the function \hat{v} by the unperturbed solution (2.10). The first term can

be expected to be small, because $u(x)$ varies little in the pulse interval, which is of $\mathcal{O}(1)$ width in $\hat{\xi}$. The second term is small if $\frac{c}{\sqrt{BD}} \ll 1$. The pulse velocity c , of course, unknown yet; naturally, in the final results, c will depend on A, B , and D . Our strategy will be to determine c under the assumption that the right-hand side of (3.16) is a perturbation and then verify a posteriori (section 3.5) under what conditions on the parameters the perturbation assumption is satisfied.

3.4. Computation and analysis of the pulse velocity. In order to carry out a leading order asymptotic analysis of the condition (3.19), $\hat{v}(\hat{\xi})$ may be replaced by the presumed first approximation $\hat{v}_0(\hat{\xi})$ given in (2.10). Also, for a single stationary pulse solution centered at $\hat{\xi} = 0$, it may be readily shown, via a calculation in the original ξ variable, that the term involving the derivative of u has the following form:

$$(3.20) \quad \frac{\partial}{\partial \hat{\xi}} \left(\frac{u}{u_0} \right) = \left[\frac{\partial}{\partial \hat{\xi}} \left(\frac{u}{u_0} \right) \right]_{\hat{\xi}=0} + \tilde{f}(\hat{\xi}) + \text{h.o.t.},$$

where $\tilde{f}(\hat{\xi})$ is an odd function of $\hat{\xi}$. In particular, for $\xi = \mathcal{O}(\sqrt{D/B})$, the by now standard approximations imply that (3.10) yields to leading order:

$$(3.21) \quad \frac{\partial u}{\partial \xi}(\xi) = \frac{-u_0}{(\mu_+ - \mu_-)} \left\{ \mu_- \int_{-\Gamma(t)}^{\xi} v^2 dx' + \mu_+ \int_{\xi}^{\infty} v^2 dx' - \mu_+ e^{-(\mu_+ - \mu_-)\Gamma} \int_{-\Gamma}^{\infty} v^2 dx' \right\}.$$

The higher order terms introduce a relative error of $\mathcal{O}(\sqrt{AD/B})$. Then, $\int_{-\Gamma}^0 v^2 \sim \int_{-\infty}^0 v^2$ and $\int_{-\Gamma}^{\xi} v^2 \sim \int_{-\infty}^{\xi} v^2$, since the tails $\int_{-\infty}^{-\Gamma} v^2$ are exponentially small. Also, the function $\hat{v}_0(\hat{\xi})$ is symmetric about $\hat{\xi} = 0$, so that $\int_{-\infty}^0 v^2 dx' = \int_0^{\infty} v^2 dx'$ to leading order. Hence, (3.21) reduces to

$$(3.22) \quad \frac{\partial u}{\partial \xi}(\xi) = \frac{ku_0}{(\mu_+ - \mu_-)} \left[\frac{c}{2} + \mu_+ e^{-(\mu_+ - \mu_-)\Gamma(t)} \right] + u_0 \tilde{f}(\xi),$$

where $\tilde{f}(\xi) \equiv \frac{1}{2} \int_{-\infty}^{\xi} v^2(x') dx' - \frac{1}{2} \int_{\xi}^{\infty} v^2(x') dx'$ and where k is defined in (3.14). Clearly, $\tilde{f}(\xi)$ is antisymmetric about $\xi = 0$. Finally, using (2.11) to evaluate k , recalling the definitions (3.8) of μ_{\pm} , converting to $\hat{\xi}$, and dividing both sides by u_0 , we get to leading order

$$(3.23) \quad \frac{\partial}{\partial \hat{\xi}} \frac{u}{u_0}(\hat{\xi}) = \frac{3BD}{u_0^2} \left\{ e^{-\sqrt{c^2+4A}\Gamma(t)} + \frac{c[1 - e^{-\sqrt{c^2+4A}\Gamma(t)}]}{\sqrt{c^2 + 4A}} \right\} + \tilde{f}(\hat{\xi}).$$

Hence, we arrive at (3.20): the first term in (3.23) is $(\partial/\partial \hat{\xi})(u/u_0)$ at $\hat{\xi} = 0$, and the second term is antisymmetric about $\hat{\xi} = 0$, as claimed above.

Since \tilde{f} is odd, the integral of $\hat{v}^3 \tilde{f}$ in (3.19) vanishes to leading order, and the condition for the existence of one-pulse solutions simplifies to

$$(3.24) \quad \frac{-c}{\sqrt{BD}} \int_{-\infty}^{\infty} \left(\frac{\partial \hat{v}_0}{\partial \hat{\xi}} \right)^2 d\hat{\xi} + \frac{1}{3} \left[\frac{\partial}{\partial \hat{\xi}} \left(\frac{u}{u_0} \right) \right]_{\hat{\xi}=0} \int_{-\infty}^{\infty} \hat{v}_0^3(\hat{\xi}) d\hat{\xi} = 0.$$

Evaluating the integrals using (2.10), one obtains

$$(3.25) \quad \frac{-c}{\sqrt{BD}} + 2 \left[\frac{\partial}{\partial \hat{\xi}} \left(\frac{u}{u_0} \right) \right]_{\hat{\xi}=0} = 0.$$

Next, the values of u_0 can be determined. Using (3.15) and (2.11), we find

$$(3.26) \quad u_0(1 - u_0) = 6 \frac{B^{3/2} \sqrt{D}}{(\mu_+ - \mu_-)} \left[1 - \left(\frac{\mu_+}{\mu_-} \right) e^{-(\mu_+ - \mu_-)\Gamma} \right].$$

Now, just as in the analysis of (2.12) in section 2, there are two cases to consider:

$$(3.27) \quad \text{Case I: } B^{3/2} \sqrt{\frac{D}{A}} \ll 1; \quad \text{Case II: } B^{3/2} \sqrt{\frac{D}{A}} = \mathcal{O}(1).$$

Moreover, in both cases, one needs to consider two possibilities: $c^2 \ll A$ and $c^2/A = \mathcal{O}(1)$. We will refer to these as subcases a and b, respectively. We analyze Case Ia in this section and Cases Ib and IIa geometrically in section 4 of Part II [1].

In Case I, the quadratic (3.26) has two real solutions, and we are interested in the smaller one:

$$(3.28) \quad (u_0)_- \sim \frac{6B^{3/2} \sqrt{D}}{(\mu_+ - \mu_-)} \left\{ 1 - \left(\frac{\mu_+}{\mu_-} \right) e^{-(\mu_+ - \mu_-)\Gamma} \right\}.$$

This solution clearly reduces to (2.14) obtained in section 2 for the case of a stationary single pulse (take $t \rightarrow \infty$, where $c = 0$). Moreover, it indicates that the method employed here, which is based on the separation of scales, is consistent if we impose the global condition $A \ll B^2$ given in (2.16). See Remark 2.1 for the interpretation of the other root u_0 just below one.

Specializing to Case Ia, we see by (3.8) that (3.23) and (3.28) simplify (to leading order) to

$$(3.29) \quad \left[\frac{\partial}{\partial \xi} \left(\frac{u}{u_0} \right) \right]_{\xi=0} = \frac{3BD}{u_0^2} e^{-2\sqrt{A}\Gamma(t)}, \quad (u_0)_- = 3\sqrt{\frac{D}{A}} B^{3/2} \left\{ 1 + e^{-2\sqrt{A}\Gamma(t)} \right\}.$$

Hence, by using (3.29) in (3.25), we get to leading order

$$(3.30) \quad c = \frac{2A\sqrt{D}}{3B^{3/2}} \frac{e^{-2\sqrt{A}\Gamma(t)}}{\left[1 + e^{-2\sqrt{A}\Gamma(t)} \right]^2},$$

where we recall (3.1) in which $\Gamma(t)$ is defined as $\Gamma(t) = \int_0^t c(s) ds$. Since $B^{3/2} \sqrt{D/A} \ll 1$ (Case I) and $A \ll B^2$ (by (2.16)), we find $c(t) \ll 1$ for (3.30). Thus, $c(t)$ corresponds to a slowly propagating pulse solution whose wave speed decreases slowly in time.

Finally, recalling (3.1), we see that (3.30) is also a differential equation:

$$(3.31) \quad \frac{d\Gamma}{dt} = \frac{2}{3} \frac{A\sqrt{D}}{B^{3/2}} \frac{e^{-2\sqrt{A}\Gamma}}{\left[1 + e^{-2\sqrt{A}\Gamma} \right]^2}.$$

There are no critical points for finite Γ in (3.31), and hence Γ grows without bound.

Equation (3.31) can be solved in an implicit form, but not much insight is gained. Instead, we finish with an ODE for $c(t)$ that can be obtained by differentiating (3.30) by t and by a little algebra (in particular, view (3.30) as a quadratic in $e^{-2\sqrt{A}\Gamma}$ and solve it, taking the root with the minus sign; then, plug this root into the right-hand side of the formula for dc/dt):

$$(3.32) \quad \frac{dc}{dt} = -2\sqrt{A}c^2 \sqrt{1 - \frac{6cB^{3/2}}{A\sqrt{D}}}.$$

Hence, $c(t)$ decreases algebraically until the wave is asymptotically stationary. In addition, there is an upper bound for $c(t)$, whose origin is geometric (see Part II).

Remark 3.1. The existence of the pairs of slowly modulated two-pulse solutions is consistent with results from [2], where it was proven that traveling waves that are stationary in a frame moving with constant nonzero speed cannot exist in the parameter regime studied there (see Remark 2.2): if the two pulses would travel forever (without splitting), then each would look like a single traveling pulse. Thus, $c(t)$ must approach 0 as $t \rightarrow \infty$.

Remark 3.2. In the numerical simulations for [2], $D = \delta^2$, $A = \mathcal{O}(\delta^2)$, $B = \mathcal{O}(\delta^{2\alpha/3})$, and typically $\alpha = 1$. Hence, (3.30) satisfies $c(t) = \mathcal{O}(A\sqrt{D}/B^{3/2}) = \mathcal{O}(\delta^2)$, as observed in Figure 9 of [2].

3.5. Consistency of the approximations and a mechanism for the pulse-splitting bifurcation. In this section, we analyze the conditions under which the right-hand side of (3.16) is indeed a perturbation. There are two terms to consider. By (3.30), it follows that $c/\sqrt{BD} = (A/B^2)\hat{c}$, where $\hat{c} = \mathcal{O}(1)$, and hence the second term on the right-hand side of (3.16) is a perturbation when (2.16) holds.

To analyze the first term, we expand $u(\hat{\xi})$ in a Taylor series:

$$(3.33) \quad \frac{u_0 - u}{u_0} = - \left[\frac{\partial}{\partial \hat{\xi}} \left(\frac{u}{u_0} \right) \right]_{\hat{\xi}=0} \hat{\xi} - \frac{1}{2} \left[\frac{\partial^2}{\partial \hat{\xi}^2} \left(\frac{u}{u_0} \right) \right]_{\hat{\xi}=0} \hat{\xi}^2 - \dots$$

The coefficient of the first term in (3.33) is given by (3.29). Next, the coefficient of the second term is readily computed to leading order from the quasi-static limit of the differential equation (3.3):

$$(3.34) \quad \left[\frac{\partial^2}{\partial \hat{\xi}^2} \left(\frac{u}{u_0} \right) \right]_{\hat{\xi}=0} = \frac{A}{4B^2} \frac{1}{[1 + e^{-2\sqrt{A}\Gamma}]^2}.$$

This leading order term comes directly from the uv^2 term in (3.3), and we note that the A term in (3.3) is higher order, because $\sqrt{AD/B} \ll 1$ in Case I by (2.16). Hence, condition (2.16) also ensures the smallness of the first term on the right of (3.16).

To conclude this section, we venture an explanation for the numerically observed phenomenon that, in a suitably chosen regime of the parameter space, a traveling pulse, *after some time*, splits into a right and a left traveling pulse. Consider B as a bifurcation parameter by setting $B^2 = \mathcal{O}(A^{1-\nu})$ with $\nu > 0$. The right-hand side of (3.16) ceases to be a perturbation as $\nu \rightarrow 0$, and our construction breaks down. So, let us suppose now that we take ν positive but small, yet such that all coefficients on the right-hand side of (3.16) are still numerically sufficiently small for the perturbation assumption to be valid. Then, as time goes on, the coefficient on the first term in the Taylor expansion becomes even smaller because $\hat{c} \rightarrow 0$ (3.30); however, the coefficient (3.34) of the second term in the Taylor expansion grows as $t \rightarrow \infty$, and in fact can grow up to four times its initial value. Moreover, the leading order coefficients on all terms of fourth, sixth, ... order in the Taylor expansion will also grow. Therefore, it can happen that, after some time, the perturbation assumption is no longer valid. See also section 5 of Part II for a more detailed discussion.

The time needed for the pulse to break up is smaller if ν is smaller, and hence B is closer to \sqrt{A} , which is precisely the threshold case discovered in [3] and observed there to agree with the splitting bifurcations in simulations. The time scale for break-up

can be estimated by the equation for $\Gamma(t)$, (3.31): the time-dependent factor in (3.34) decreases from being near 1 to being $\ll 1$ when $\sqrt{A}\Gamma \gg 1$ on a time scale

$$(3.35) \quad \tau = (A\sqrt{AD}/B\sqrt{B})t$$

(see also section 3.4 of Part II). However, $\Gamma(t)$ only grows logarithmically slow on this time scale (by (3.31)). Therefore, the actual splitting will occur after a very long, but $\mathcal{O}(1)$, time T_{split} on this τ time scale. For instance, with A , B , and D as in the simulations of Figure 2(b), we find that $t \approx 175\tau$ so that $T_{\text{split}} \approx 40\tau$. This agrees qualitatively with the dynamics of (3.31).

4. Stability analysis for slowly modulated two-pulse solutions. This section is organized as follows. In section 4.1, we state the scaled fourth-order eigenvalue problem. In section 4.2, we treat Case I by reducing the full problem to a second-order nonlocal eigenvalue problem and analyzing this reduced system.

4.1. The scaled fourth-order eigenvalue problem. The Gray–Scott model (1.1) written in the unscaled modulated traveling wave variable is

$$(4.1) \quad U_t = U_{\xi\xi} + c(t)U_{\xi} - UV^2 + A(1 - U), \quad V_t = DV_{\xi\xi} + c(t)V_{\xi} + UV^2 - BV.$$

Let $(u_0(\xi), v_0(\xi))$ denote a quasi-stationary, slowly modulated two-pulse solution, where the $c(t)$ dependence is implicit. Stability with respect to small perturbations is determined by setting

$$(4.2) \quad U(\xi, t) = u_0(\xi) + u(\xi)e^{\lambda t} \quad \text{and} \quad V(\xi, t) = v_0(\xi) + v(\xi)e^{\lambda t},$$

and then by studying the linearized eigenvalue problem

$$(4.3) \quad \begin{aligned} \lambda u &= u_{\xi\xi} + cu_{\xi} - v_0^2 u - 2u_0 v_0 v - Au, \\ \lambda v &= Dv_{\xi\xi} + cv_{\xi} + v_0^2 u + 2u_0 v_0 v - Bv. \end{aligned}$$

As was shown in [3] for the stability of the stationary solutions, the significant scaling of the variables in this eigenvalue problem is the same as that used in the existence analysis. Recalling (2.15), (3.30), and (3.6), let

$$(4.4) \quad \xi = \sqrt{\frac{D}{B}}\hat{\xi}, \quad u(\xi) = B^{3/2}\sqrt{\frac{D}{A}}\hat{u}(\hat{\xi}), \quad v(\xi) = \sqrt{\frac{A}{BD}}\hat{v}(\hat{\xi}), \quad c = \frac{A\sqrt{D}}{B^{3/2}}\hat{c},$$

so the eigenvalue problem (4.3) becomes

$$(4.5) \quad \begin{aligned} \hat{u}_{\hat{\xi}\hat{\xi}} &= \frac{A}{B^2} \left[(\hat{v}_0^2 \hat{u} + 2\hat{u}_0 \hat{v}_0 \hat{v}) + BD \left(1 + \frac{1}{A} \lambda \right) \hat{u} - D\hat{c}\hat{u}_{\hat{\xi}} \right], \\ \hat{v}_{\hat{\xi}\hat{\xi}} + \left[2\hat{u}_0 \hat{v}_0 - \left(1 + \frac{\lambda}{B} \right) \right] \hat{v} &= -\hat{v}_0^2 \hat{u} - \frac{A}{B^2} \hat{c}\hat{v}_{\hat{\xi}}, \end{aligned}$$

where we have used the same scalings for u_0 and v_0 . Finally, we scale the eigenvalue

$$(4.6) \quad \lambda = B\hat{\lambda}$$

(see the appendix of [3]), and, in the stability analysis, we use

$$(4.7) \quad \varepsilon = \sqrt{A}/B \ll 1 \quad \text{and} \quad \delta = \sqrt{BD} \ll 1$$

with $\delta/\varepsilon \leq \mathcal{O}(1)$. Therefore, dropping hats, we arrive at the final form of the eigenvalue problem to be studied in this section:

$$(4.8) \quad \begin{aligned} \text{(a)} \quad u_{\xi\xi} &= \varepsilon^2 (v_0^2 u + 2u_0 v_0 v) + \varepsilon^2 \delta^2 u + D\lambda u - \varepsilon^2 Dcu_{\xi}, \\ \text{(b)} \quad v_{\xi\xi} + [2u_0 v_0 - (1 + \lambda)] v &= -v_0^2 u - \varepsilon^2 cv_{\xi}. \end{aligned}$$

4.2. Transformation of (4.8) to a second-order NLEP. In this section, we reduce the full fourth-order eigenvalue problem (4.8) to a second-order NLEP. This analysis extends to the $c(t) > 0$ case the procedure for deriving an NLEP previously introduced in [3] for the $c = 0$ case. In this section we will assume that $D \ll 1$; as a consequence we will find that the first derivative terms with factors of $c(t)$ in them are of higher order. This simplifies the analysis considerably. The case $D \geq \mathcal{O}(1)$ is discussed in Remark 4.2.

The essence of the procedure for deriving the NLEP is to exploit the fast/slow structure of the underlying quasi-stationary solution to determine the fast/slow structure of the eigenfunctions. We recall that $v_0(\xi)$ is exponentially small in the slow regimes. Hence, (4.8)(a) reduces to

$$(4.9) \quad u_{\xi\xi} = \varepsilon^2 \delta^2 u + D\lambda u - \varepsilon^2 Dc u_\xi + \text{expo. small.}$$

Therefore, the u component of the eigenfunction consists of slow segments along which u undergoes slow exponential decay as $|x| \rightarrow \infty$, and there is also a jump discontinuity in u_ξ across $\xi = 0$, since there is a difference between the slopes of the right and left slow solutions as $|\xi|$ approaches zero. We label this jump discontinuity in the slow field by $\Delta_s u_\xi$, and it plays an essential role, as we saw in [3].

To determine the leading order behavior of $\Delta_s u_\xi$, we analyze the terms in the slow u equation (4.9). The third term on the right is always subdominant to the second, because $\varepsilon \ll 1$. The dominant term is then either the second or the first term, or both, depending on whether one is in

$$\text{Regime 1: } \varepsilon^2 \delta^2 \ll D, \quad \text{Regime 2: } \varepsilon^2 \delta^2 \gg D, \quad \text{or} \quad \text{Regime 3: } \frac{\varepsilon^2 \delta^2}{D} = \mathcal{O}(1),$$

Remark 4.1. It must be noted that $\varepsilon^2 \delta^2 = AD/B$. In other words, these three regimes are more simply defined by $A \ll B$, $A \gg B$, and $A/B = \mathcal{O}(1)$.

Next, we recall that the fast regime is a narrow interval about $\xi = 0$ and, in this interval, $v_0(\xi)$ possesses a pulse, while u_0 is an $\mathcal{O}(1)$ constant as function of ξ , at leading order (see (3.29) and use (4.4)). Hence, to leading order in the fast regime, $u_{\xi\xi} = \varepsilon^2(v_0^2 u + 2u_0 v_0 v) + D\lambda u$, which implies that the u component of the eigenfunction is constant to leading order for $\varepsilon \ll 1$ and for small D . We label this constant κ . Moreover, the derivative u_ξ has a jump discontinuity:

$$(4.10) \quad \Delta_f u_\xi = \varepsilon^2 \int_{-\infty}^{\infty} (uv_0^2 + 2u_0 v_0 v) d\xi + D\lambda \int_{-\infty}^{\infty} u d\xi + \text{h.o.t.}$$

Here, we note that the limits have been obtained from the appropriate (exact) ε - and δ -dependent times at which the pulse enters and exits the fast field and from then sending ε and $\delta \rightarrow 0$. Hence, the integral of the constant has a finite value (see [3, 4]).

Finally, the transformation to the NLEP is completed by determining the constant κ . This is now done on a regime-by-regime basis for different regimes in the ε - δ - D parameter space. We will match the jump discontinuities $\Delta_s u_x$ and $\Delta_f u_\xi$, as computed in the slow and fast fields, respectively, and obtain formulae for κ . Different terms will be of leading order in different regimes.

Remark 4.2. The stability of the stationary one-pulse patterns (see section 2) follows immediately from the results in this section by setting $c \equiv 0$. As a consequence, we do not have to assume that $D \ll 1$ when studying these one-pulse patterns. The case $D \geq \mathcal{O}(1)$ is a subcase of Regime 1. We will find in section 4.2.1 that the pulse

patterns are always unstable for $\varepsilon^2 \ll \sqrt{D}$, i.e., that there cannot be stable pulse solutions when $D \geq \mathcal{O}(1)$ (in the parameter regime studied in this paper; see Remark 1.1). By construction, the modulated two-pulse solutions evolve toward two copies of these stationary one-pulse solutions as $t \rightarrow \infty$. Therefore, it is of only limited relevance to consider the case $D \geq \mathcal{O}(1)$ for the modulated two-pulse patterns, since these solutions cannot be stable (at least not for t large); see also section 3.4 of Part II [1].

4.2.1. Regime 1. In this section, we treat Regime 1 in detail. Since $\varepsilon^2 \delta^2 \ll D$, (4.9) implies that the left and right slow segments of u are given (in terms of the fast variable) to leading order by

$$(4.11) \quad u(\xi) = \kappa e^{\pm\sqrt{D}\lambda\xi}.$$

Hence, between the left and right slow solutions, $\Delta_s u_\xi$ is to leading order:

$$(4.12) \quad \Delta_s u_\xi = \lim_{\xi \rightarrow 0^-} u_\xi - \lim_{\xi \rightarrow 0^+} u_\xi = -2\sqrt{D}\lambda\kappa.$$

In order to match this slow jump discontinuity to the fast jump discontinuity $\Delta_f u_\xi$ given by (4.10), we first assume $\varepsilon^2 \gg D$, so that the first term in the right-hand side of (4.10) is the dominant term. This is done largely to facilitate the analysis, and the complementary regime ($\varepsilon^2/D \leq \mathcal{O}(1)$) will be treated at the end of this section. The explicit leading order matching condition needed to determine κ is

$$(4.13) \quad -2\sqrt{D}\lambda\kappa = \varepsilon^2 \left[\kappa \int_{-\infty}^{\infty} v_0^2 d\xi + 2u_0 \int_{-\infty}^{\infty} v_0 v d\xi \right].$$

Since the scaling included the assumption $\lambda = \mathcal{O}(1)$, there are three subregimes to consider:

$$(4.14) \quad \text{1a: } \varepsilon^2 \ll \sqrt{D}, \quad \text{1b: } \varepsilon^2 = \mathcal{O}(\sqrt{D}), \quad \text{1c: } \varepsilon^2 \gg \sqrt{D}.$$

In subregime 1a, the matching condition (4.13) directly yields $\kappa = \mathcal{O}(\varepsilon^2/\sqrt{D}) \ll 1$; i.e., the constant value of u to leading order during the fast jump is asymptotically small. Hence, the coupling of the slow field to the fast field is weak (i.e., of higher order), and the leading order fast eigenvalue problem is precisely that associated with a single isolated fast homoclinic pulse,

$$v_{\xi\xi} + [2u_0 v_0 - (1 + \lambda)]v = 0,$$

which has a (scaled) positive eigenvalue at $\lambda = 5/4$. Therefore, since the higher order terms will displace this eigenvalue only by a small amount, there exists an eigendirection along which small perturbations lead to exponential growth, and these solutions are formally unstable in subregime 1a.

In subregime 1b, where $\varepsilon^2 = \mathcal{O}(\sqrt{D})$, we introduce the new $\mathcal{O}(1)$ parameter,

$$(4.15) \quad d = \frac{\sqrt{D}}{\varepsilon^2},$$

and remark that $d = \sqrt{D}B^2/A$ in the original parameters. All of the terms in the leading order matching condition (4.13) are now retained, and one finds

$$(4.16) \quad \kappa = \frac{-u_0^3}{3 + d\sqrt{\lambda}u_0^2} \int_{-\infty}^{\infty} v_0(\xi)v(\xi)d\xi.$$

Here we have again used $\int_{-\infty}^{\infty} v_0^2(\xi)d\xi = 6/u_0^2$. Clearly, this value of κ is of $\mathcal{O}(1)$, since d, u_0 , and λ are $\mathcal{O}(1)$. Hence, by replacing the variable u with its leading order constant value κ over the fast field on the right-hand side of the second equation in (4.8), by neglecting the higher order cv_ξ term, and by recalling κ from (4.16), we find that the leading order eigenvalue problem becomes

$$(4.17) \quad v_{\xi\xi} + [2u_0v_0 - (1 + \lambda)]v = -\kappa v_0^2.$$

This turns out to be exactly the same NLEP analyzed in Case II of section 5.2 in [3] ($\beta = 1/2$), which is the significant scaling in which the solutions gain stability through a Hopf bifurcation. (This is not surprising since the parameters A, B, D are also related by $\varepsilon^2 = A/B^2 = \mathcal{O}(\sqrt{D})$ for $\beta = 1/2$ in [3].) To make this correspondence precise, we introduce a new parameter $\ell = \ell(t)$ via $u_0 = 3\ell$, where $u_0 = (\hat{u}_0)_-$ is given by (3.29) and (4.4). This new parameter will help greatly to keep the algebra to a minimum. Explicitly,

$$(4.18) \quad \ell = 1 + e^{-2\sqrt{A}\Gamma(t)}.$$

Hence, we know $\ell \in (1, 2)$ for all $0 < \Gamma(t) < \infty$, since $\ell \rightarrow 2$ as $\Gamma \downarrow 0$, $\ell \rightarrow 1$ as $\Gamma \rightarrow \infty$, and ℓ is a monotonically decreasing function of Γ .

Next, we follow the procedure used in section 5 in [3] and change the independent and dependent variables and parameters in the NLEP (4.17). Let $t = \xi/2, y(t) = v(\xi)$,

$$(4.19) \quad P^2 = 4(1 + \lambda) \quad \text{and} \quad C = \frac{9}{1 + 3d\ell^2\sqrt{\lambda}}.$$

The NLEP (4.17) then becomes

$$(4.20) \quad \ddot{y} + [12\text{sech}^2(t) - P^2]y = C\text{sech}^4(t) \int_{-\infty}^{\infty} y(t)\text{sech}^2(t)dt,$$

where $\dot{} = d/dt$, and we used $v_0(\xi) = (3/2u_0)\text{sech}^2(\xi/2)$ and $u_0 = 3\ell$. Inverting the formula for C , we get

$$(4.21) \quad d\ell^2(t) = \frac{2}{3\sqrt{P^2 - 4}} \left[\frac{9}{\mathcal{C}(P)} - 1 \right],$$

where $\mathcal{C}(P)$ is an explicitly known expression in terms of integrals over hypergeometric functions; see section 5.1 in [3] for the derivation of $\mathcal{C}(P)$. This formula should be interpreted as follows: An eigenvalue λ of (4.8) corresponds by (4.19) to a solution P of (4.21). Note that this implies that $\lambda = \lambda(t)$, i.e., that the eigenvalues λ of the linearized stability problem (4.8) vary on the same slow time scale τ (3.35) as (half) the distance between the pulses Γ .

Formula (4.21) is identical to formula (5.15) from [3] with $a = \sigma = m = 1$ and $b^2 = d\ell^2(t)$. Therefore, it follows from the hypergeometric functions analysis in [3] (see (5.16) and Figure 5 in [3]) that there are no eigenvalues λ with $\text{Re}(\lambda) > 0$ when

$$(4.22) \quad d\ell^2(t) \leq d_H \approx (0.66)^2 \approx 0.44.$$

Since $\ell(t)$ decreases monotonically from 2 to 1, we can conclude that the modulated two-pulse solutions are formally stable for all t when

$$(4.23) \quad d \leq \frac{d_H}{4} \approx 0.11, \quad \text{i.e.,} \quad D < 0.012 \dots \varepsilon^2 \quad \text{or} \quad DB^4 < 0.012 \dots A$$

(by (4.15), (4.7)). Moreover, all modulated two-pulse solutions (including the limiting stationary one-pulse solutions) are unstable when

$$(4.24) \quad d \geq d_H \approx 0.44, \quad \text{i.e., } D > 0.19 \dots \varepsilon^2 \text{ or } DB^4 > 0.19 \dots A.$$

For $0.11 < d < 0.44$, i.e., $0.012\varepsilon^2 < D < 0.19\varepsilon^2$, the situation is more “dynamic.” We know from [3] that there are no eigenvalues $\lambda(t)$ with $\text{Re}(\lambda(t)) > 0$ when $d\ell^2(t) \leq d_H$ (4.22); moreover, there are two unstable eigenvalues when $d\ell^2(t) > d_H$. Therefore, we define for a given $d \in (d_H/4, d_H) \approx (0.11, 0.44)$ a critical value of ℓ , $1 < \ell_* < 2$, such that $d\ell_*^2 = d_H \approx 0.44$. The modulated two-pulse solution is then stable for all $t > t_*$, where t_* is defined by $\ell(t_*) = \ell_*$, since both eigenvalues have crossed the imaginary axis at $t = t_*$. Equivalently, it is unstable for $t < t_*$. Note that this implies that the limiting solutions, the stationary one-pulse solutions, are stable for all $d < d_H$. However, a pair of two-pulse solutions will be stable (i.e., numerically observable) only for $d \in (d_H/4, d_H)$ when the distance between the two pulses is “large enough.”

The bifurcation at which the two eigenvalues cross the imaginary axis is a Hopf bifurcation: the eigenvalues are a complex conjugate pair and purely imaginary at the bifurcation. These two eigenvalues merge and become real as d , or $d\ell^2$, is increased; see again [3] for explicit calculations. In the limit $d \gg 1$, i.e., in the transition from Regime 1b to Regime 1a, one of these eigenvalues will approach $5/4$ and the other decreases towards 0. Thus, we have recovered the instability result of Regime 1a and deduced the existence of a second unstable eigenvalue near 0 in this case. Using (4.21) we can write an explicit approximation for this eigenvalue using the fact that $\mathcal{C}(P) \rightarrow 9/2$ as $P \rightarrow 2$, i.e., that $\lambda \rightarrow 0$ by (4.19) (see [3]): for $d \gg 1$ to leading order,

$$(4.25) \quad \lambda(t) = \frac{4}{9d\ell^4(t)} \ll 1 \quad \text{or} \quad \lambda(t) = \frac{4}{9\ell^2(t)} \frac{\varepsilon^4}{D} \ll 1.$$

This eigenvalue will yield the instability result when $D \geq \varepsilon^2$ (see below).

Next, we turn to Regime 1c. The stability result of Regime 1b, (4.23), can be extended into this regime in a natural fashion, since $d \ll d_H/4$ in Regime 1c. Thus, since $\sqrt{D} \ll \varepsilon^2$ we can take the limit $d \rightarrow 0$ in (4.16) and derive

$$(4.26) \quad \kappa = \frac{-u_0^3}{3} \int_{-\infty}^{\infty} v_0(\xi)v(\xi)d\xi;$$

i.e., the left-hand side of (4.13), the slow jump in u_ξ , has become of higher order compared to the right-hand side, the fast jump in u_ξ . It follows from the analysis in [3] that both eigenvalues that crossed the imaginary axis in Regime 1b remain at the stable side of this axis in this limit. In fact, with this value of κ , the NLEP (4.17) is the same as that derived in Case III of section 5.2 in [3], namely, in the regime where the parameter β satisfies $1/2 < \beta < 1$. Hence, we may conclude directly that all the slowly modulated two-pulse solutions are formally stable.

Finally, in Regime 1, we skipped the case $D \geq \mathcal{O}(\varepsilon^2)$, which includes the case $D \geq \mathcal{O}(1)$. Here, we do get the same instability result as in Regime 1a. However, the instability is not caused by the unstable eigenvalue found near $5/4$. This eigenvalue cannot exist when $D \gg \varepsilon^2$, since then the u -component of the eigenvalue problem (4.8) is given by $u_{\xi\xi} = D\lambda u$ at leading order, both in the fast field and in the slow field. Therefore, there are for $\lambda = \mathcal{O}(1)$ no eigenfunctions that are bounded as $|x| \rightarrow \infty$. Nevertheless, the eigenvalue of $\mathcal{O}(\varepsilon^4/D) \ll 1$ with $\lambda \ll 1$, (4.25), is still there. It is not influenced by the fact that $D \gg \varepsilon^2$ since the term $D\lambda u$ is once again only

of higher order (in the fast field) for a λ of this magnitude. We may conclude that the unstable eigenvalue (4.25) exists for all $D \geq \mathcal{O}(\varepsilon^2)$ and thus that the slowly modulating two-pulse solutions are also formally unstable in this part of Regime 1.

4.2.2. Regime 2. In this regime, $D \ll \varepsilon^2 \delta^2$, so that the first equation (4.9) is to leading order $u_{\xi\xi} = \varepsilon^2 \delta^2 u$. Hence, the left and right slow segments (expressed in terms of the fast variable) are to leading order $u(\xi) = \kappa e^{\pm \varepsilon \delta \xi}$, and the leading order jump discontinuity in u_ξ at $x = 0$ between them is

$$(4.27) \quad \Delta_s u_\xi = -2\varepsilon \delta \kappa.$$

The corresponding jump discontinuity at $x = 0$ in the fast field is given by the first term in (4.10):

$$(4.28) \quad \Delta_f u_\xi = \varepsilon^2 \int_{-\infty}^{\infty} (\kappa v_0^2 + 2u_0 v_0 v) d\xi.$$

Finally, matching these leading order jump discontinuities, i.e., equating (4.27) and (4.28) and recalling $\delta/\varepsilon \ll 1$, we recover (4.26). This is not surprising since, as in Regime 1c, $\Delta_s u_\xi \ll \Delta_f u_\xi$. Thus, as in Regime 1c, we can immediately conclude that the slowly modulating two-pulse solutions are linearly stable in Regime 2 by referring to the analysis for Case III in section 5.3 of [3].

4.2.3. Regime 3. In this final regime, $\varepsilon^2 \delta^2 / D = \mathcal{O}(1)$, and we introduce the new $\mathcal{O}(1)$ parameter $s = \varepsilon^2 \delta^2 / D$. The slow eigenvalue problem (4.9) becomes to leading order $u_{\xi\xi} = D(s + \lambda)u$, and hence the relevant jump discontinuity is

$$(4.29) \quad \Delta_s u_\xi = -2\sqrt{D(s + \lambda)}\kappa.$$

The jump in u_ξ in the fast field is still given by (4.10). Therefore, the matching condition is

$$(4.30) \quad -2\sqrt{D(s + \lambda)}\kappa = \varepsilon^2 \int_{-\infty}^{\infty} (uv_0^2 + 2u_0 v_0 v) d\xi + D\lambda \int_{-\infty}^{\infty} u d\xi + \text{h.o.t.}$$

There are three subregimes (as in Regime 1), and the analysis proceeds in the same fashion. The results from Regime 1 may be applied directly here after taking into account the shift in the spectrum by the parameter-dependent amount s .

Remark 4.3. Although we divided the parameter space into (sub)regimes, there is only one, namely, Regime 1b, where $\varepsilon^2 = \mathcal{O}(\sqrt{D})$ and in which there is a transition from stable to unstable. Hence, we have the curve $\mathcal{C}_{\text{HOPF}}$ in Figure 2 of Part II [1].

5. Discussion. The analysis of two-pulse solutions in this paper can be interpreted as a study of “mildly strongly” coupled pulses in singular perturbed R-D equations. This coupling is “mildly strong,” since the U -components of the solutions are not assumed to be close to the trivial state $U = 1$ and, in fact, vary by $\mathcal{O}(1)$ amounts. Hence, the interaction between the two modulating pulses is stronger than that which occurs only via exponentially small “tail interactions.”

As was shown in section 3 for Case Ia, the separation distance $2\Gamma(t)$ obeys a highly nonlinear ODE (3.31) that is valid for any $\mathcal{O}(1)$ Γ . The denominator of the vector field in (3.31) is important for accurately describing the rate of change of Γ for small to medium values of Γ , while the numerator captures the long-term dynamics to leading order after Γ has become sufficiently large. In terms of the scaling (3.35),

$\Gamma(\tau)$ has become sufficiently large already when $\Gamma(\tau) = \mathcal{O}(\ln \tau)$ with $\tau \gg 1$. In this regime, the ODE (3.31) reduces to

$$(5.1) \quad \frac{d\Gamma}{d\tau} = \frac{2}{3\sqrt{A}} e^{-2\sqrt{A}\Gamma(\tau)},$$

which is precisely the equation that is appropriate for describing weakly coupled pulses, since $U_{\max}(\tau)$ has approached $U = 1$ and $c(t)$ has become $\ll 1$. Moreover, translating this equation for the weak interaction limit into an equation written in terms of the scaled speed $\hat{c}(\tau)$, one gets to leading order $d\hat{c}/d\tau = -2\hat{c}^2$, which is a significantly simplified version of (3.32), for mildly strong interactions.

Remark 5.1. Equation (5.1) valid for sufficiently large Γ agrees with the equation determined concurrently in [8] for pulse interactions in (1.1). The results in [8] apply to more general equations which satisfy the requirement that the separation distance between the two pulses exceeds some threshold so that the concentrations of all species are exponentially close to their homogeneous steady state values.

Acknowledgments. We thank Paul Zegeling for useful conversations and D. Morgan for help in making the figures. Wiktor Eckhaus thanks his coauthors for introducing him to this problem.

REFERENCES

- [1] A. DOELMAN, W. ECKHAUS, AND T.J. KAPER, *Slowly modulated two-pulse solutions in the Gray–Scott model II: Geometric theory, bifurcations, and splitting dynamics*, SIAM J. Appl. Math., to appear.
- [2] A. DOELMAN, T.J. KAPER, AND P. ZEGELING, *Pattern formation in the one-dimensional Gray–Scott model*, Nonlinearity, 10 (1997), pp. 523–563.
- [3] A. DOELMAN, R.A. GARDNER, AND T.J. KAPER, *Stability analysis of singular patterns in the 1-D Gray–Scott model: A matched asymptotics approach*, Phys. D, 122 (1998), pp. 1–36.
- [4] A. DOELMAN, R.A. GARDNER, AND T.J. KAPER, *A stability index analysis of 1-D patterns of the Gray–Scott model*, Mem. Amer. Math. Soc., to appear.
- [5] A. DOELMAN, R.A. GARDNER, AND T.J. KAPER, *Large stable pulse solutions in reaction-diffusion equations*, Indiana Univ. Math. J., 49 (2000).
- [6] W. ECKHAUS, *Asymptotic Analysis of Singular Perturbations*, North-Holland, Amsterdam, 1979.
- [7] W. ECKHAUS AND R. KUSKE, *Pattern formation in systems with slowly varying geometry*, SIAM J. Appl. Math., 57 (1997), pp. 112–152.
- [8] S. EI, Y. NISHIURA, AND B. SANDSTEDT, *Pulse-interaction approach to self-replicating dynamics in reaction-diffusion systems*, in preparation.
- [9] C. ELPHICK, A. HAGBERG, AND E. MERON, *Dynamical front transitions and spiral vortex nucleation*, Phys. Rev. E, 51 (1995), pp. 3052–3058.
- [10] P. GRAY AND S.K. SCOTT, *Autocatalytic reactions in the isothermal, continuous stirred tank reactor: Oscillations and instabilities in the system $A + 2B \rightarrow 3B$, $B \rightarrow C$* , Chem. Engrg. Sci., 39 (1984), pp. 1087–1097.
- [11] J.K. HALE, L.A. PELETIER, AND W.C. TROY, *Exact homoclinic and heteroclinic solutions of the Gray–Scott model for autocatalysis*, SIAM J. Appl. Math., 61 (2000), pp. 102–130.
- [12] J.K. HALE, L.A. PELETIER, AND W.C. TROY, *Stability and instability in the Gray–Scott model: The case of equal diffusivities*, Appl. Math. Lett., 12 (1999), pp. 59–65.
- [13] K.J. LEE AND H.L. SWINNEY, *Lamellar structures and self-replicating spots in a reaction-diffusion system*, Phys. Rev. E, 51 (1995), pp. 1899–1915.
- [14] K.-J. LIN, W.D. MCCORMICK, J.E. PEARSON, AND H.L. SWINNEY, *Experimental observation of self-replicating spots in a reaction-diffusion system*, Nature, 369 (1994), pp. 215–218.
- [15] D.S. MORGAN, A. DOELMAN, AND T.J. KAPER, *Stationary periodic orbits in the 1-D Gray–Scott model*, Meth. Appl. Anal., 7 (2000), pp. 105–150.
- [16] C. MURATOV AND V. OSIPOV, *Spike Autosolitons in the Gray–Scott Model*, preprint, 1998.
- [17] Y. NISHIURA AND D. UEYAMA, *A skeleton structure for self-replication dynamics*, Phys. D, 130 (1999), pp. 73–104.

- [18] J.E. PEARSON, *Complex patterns in a simple system*, Science, 261 (1993), pp. 189–192.
- [19] V. PETROV, S.K. SCOTT, AND K. SHOWALTER, *Excitability, wave reflection, and wave splitting in a cubic autocatalysis reaction-diffusion system*, Philos. Trans. Roy. Soc. London, Ser. A, 347 (1994), pp. 631–642.
- [20] W.N. REYNOLDS, J.E. PEARSON, AND S. PONCE-DAWSON, *Dynamics of self-replicating patterns in reaction diffusion systems*, Phys. Rev. Lett., 72 (1994), pp. 2797–2800.
- [21] W.N. REYNOLDS, S. PONCE-DAWSON, AND J.E. PEARSON, *Self-replicating spots in reaction-diffusion systems*, Phys. Rev. E, 56 (1997), pp. 185–198.
- [22] A. VAN HARTEN, *Nonlinear singular perturbation problems: Proofs of correctness of a formal approximation based on a contraction principle in a Banach space*, J. Math. Anal. Appl., 65 (1978), pp. 126–168.